Data-Writing and Shifting Processes Toward a Vertical Domain Wall Motion Memory

Feifan Ye[1], Heechan Jang[1], Yoichi Shiota[1,2], Hideki Narita[1], Ryusuke Hisatomi[1,2], Shutaro Karube[1,2], Satoshi Sugimoto[3], Shinya Kasai[3], and Teruo Ono[1,2]

[1] Institute for Chemical Research, Kyoto University, Gokasho, Uji, Kyoto 611-0011, Japan
[2] Center for Spintronics Research Network, Kyoto University, Gokasho, Uji, Kyoto 611-0011, Japan
[3] National Institute for Materials Science (NIMS), 1-2-1 Sengen, Tsukuba, Ibaraki 305-0047, Japan

We demonstrate data writing and shifting processes in a double-free-layer nanopillar with perpendicular magnetic anisotropy. For the data writing process, the magnetization of the lower free layer is switched by injecting in-plane current pulses into the Pt bottom electrode to generate spin-orbit torque. The written information, i.e., the magnetization direction of the lower free layer, is subsequently transferred to the upper free layer through spin-transfer torque by injecting out-of-plane current pulses into the nanopillar. Furthermore, we verify that this write-and-shift memory operation can be achieved from different initial magnetization states.

Index Terms—**domain wall motion memory, 3D memory, spin-orbit torque, spin-transfer torque, magnetization switching.**

I. INTRODUCTION

THE cell of a domain wall (DW) motion memory is typically a ferromagnetic nanowire, where the data is stored by the magnetization orientation of magnetic domains separated by DWs [1]-[3]. By injecting current pulses into the nanowire, the position of DWs can be moved within the nanowire through spin-transfer torque (STT) originated from the s-d interaction between conducting electrons and the magnetization in the material [4]-[6]. Due to the rapid movement of DWs, DW motion memory can achieve fast operation speeds [7]. These advantages could make the DW motion memory a potential alternative to existing storage technologies.

However, traditional DW motion memory still faces several challenges for practical applications. First, there is a dilemma between thermal stability and power consumption, as a high energy barrier for data stability inevitably leads to a larger critical current density (J_c) required to move DWs [8]. Moreover, to meet the growing demand for higher integration density in the post-Moore's Law era, it is crucial to enhance the bit density per unit area on the chip [9], [10]. Nevertheless, traditional 2D structures of DW motion memory face substantial challenges in effective scaling while maintaining optimal performance, thereby limiting their potential to achieve greater integration density.

FIG. 1 HERE

To tackle this challenge, we proposed a novel vertical domain wall motion memory with perpendicular magnetic anisotropy (PMA), as shown in Fig. 1. In this type of memory cell, data writing is achieved by injecting in-plane current pulses into a heavy-metal bottom electrode, which induces spin-orbit torque (SOT) to switch the magnetization of the bottom-most ferromagnetic layer [11]-[14]. Subsequently, out-of-plane current pulses are injected to transfer the data bits to the upper layer via spin transfer torque (STT). Micromagnetic simulations have shown that by carefully selecting combinations of magnetic materials for storage and DW layers,

we can achieve both high thermal stability and low J_c [15], [16]. Additionally, the vertical memory structure makes high-density 3D array integration possible [17], [18].

To realize the above-mentioned vertical DW memory devices, it is essential to demonstrate data-writing and shifting operation within a single device. Although previous research has made some progress in probabilistic computing using double-free-layer devices [19]-[21], no reports to date have described a write-and-shift memory operation. In this study, we fabricated double-free-layer nanopillars with a diameter of 300 nm. Then, we investigated the data-writing and shifting processes in the nanopillar to show the feasibility of the vertical memory structure.

II. EXPERIMENTAL RESULTS

A. Device Fabrication

Multilayers of Ta(5) / Pt(10) / Co(1.2) / Cu(3) / Co(t_{Co}) / Pt(t_{Pt}) / Co(t_{Co}) / Cu(3) / Pt(3) with wedge-shaped Co and Pt were deposited on thermally oxidized Si substrate using magnetron sputtering, as shown in Fig. 2 (a). The numbers in parentheses represent the thickness of each layer in nanometers. A 10-nm-thick Pt layer was selected for the bottom electrode to induce SOT [22]-[24]. A 3-nm-thick Cu layer serves as a spacer between two free layers and allows the magnetization configuration to be identified by the giant magnetoresistance (GMR) effect.

FIG. 2 HERE

The film was fabricated into nanopillars with 300 nm diameter by electron beam lithography and Ar ion etching. The Pt bottom layer was patterned into a 2-μm-wide stripe, and the rest of the layers were etched to form a nanopillar on the Pt bottom layer. The etching depth was monitored by in-situ secondary ion mass spectroscopy for the end point detection.

Figure 2 (b) shows the memory operations we aim to perform in this study. First, in-plane current pulses are injected through the bottom Pt electrode to switch the magnetization of the Co free layer (FL1) by SOT. Then, the magnetization of the

Co/Pt/Co top free layer (FL2) is switched by out-of-plane current pulse injection without the external magnetic field.

FIG. 3 HERE

A nanopillar with thicknesses of $t_{Co} = 0.35$ nm and $t_{Pt} = 0.75$ nm was employed for the subsequent measurements. We measured the GMR properties of the nanopillar by sweeping an out-of-plane magnetic field to confirm the parallel and antiparallel magnetization states. The experimental setup is shown in Fig. 3 (a). Figure 3 (b) presents the result of GMR resistance R_{GMR} as functions of the out-of-plane magnetic field under a DC current of 0.5 mA. We observed the low-resistance and high-resistance states corresponding to parallel and antiparallel magnetization configuration, respectively. Sharp resistance changes indicate that both the free layers are aligned with the out-of-plane direction due to the sufficiently large PMA.

B. SOT-Induced Magnetization Switching

We first attempted SOT-induced magnetization switching to verify whether the magnetization of the FL1 could be reversed in the writing process. In the experiments, in-plane current pulses with a pulse duration of 20 ms were injected to the bottom Pt electrode to generate spin current by spin-Hall effect. The magnetization was initialized by applying a 300 mT out-of-plane magnetic field before measurements, and the resistance of the nanopillar was measured under a 0.5 mA DC current by GMR effect. An in-plane magnetic field of 100 mT was applied along the +x direction to break the mirror symmetry [25], [26]. However, the resistance of the nanopillar showed no significant change after the current pulse injection, which might be attributed to the insufficient torque to induce magnetization switching. To address this issue, we replaced the in-plane magnetic field with a tilted 100 mT magnetic field, thereby introducing an out-of-plane magnetic field component to facilitate SOT-induced magnetization switching. The tilted field angle θ was set to -30° when the current pulses are in the +x direction, and +30° when the current pulses are in the -x direction. The magnitude of the magnetic field component in the x-direction is 87 mT, and the magnitude of the magnetic field component in the z-direction is 50 mT. Then, we injected current pulses and plotted the results measured by GMR in Fig. 4. The resistance change of the SOT switching loop is almost identical in magnitude to that observed in the hysteresis measurement. This indicates that the magnetizations of the two free layers are antiparallel, and that the magnetization of the FL1 can be switched by SOT assisted by the tilted magnetic field. It is worth noting that when we injected current pulses in the -x direction with an initial up-up state and a tilted field angle θ of -30°, we did not observe any switching signal. This indicated that the magnetization was not reversed by the combination of the z-component of the tilted magnetic field and the Joule heating, which is independent of the direction of the current pulse.

FIG. 4 HERE

C. Data-Writing and Shifting Processes

Next, we performed experiments on data writing and shifting processes. The experiments were conducted in the following steps: First, we aligned the magnetization of the two free layers in a parallel configuration using an external out-of-plane magnetic field and then performed SOT-induced magnetization switching of the FL1 using a tilted magnetic field to achieve data writing. Next, we injected -z current pulses into the nanopillar to transfer the writing information to the FL2. Finally, to confirm the state obtained after the data shift, we measured the resistance of the nanopillar while sweeping an out-of-plane magnetic field.

FIG. 5 HERE

We conducted the above experiments with different initial states (up-up and down-down magnetization configurations), and the results are summarized in Fig. 5. We illustrate these results with the example of the up-up initial state. In the data writing step, a tilted magnetic field with a -30° elevation angle was applied. We observed a jump in the resistance of the nanopillar when a 16 mA in-plane current pulse was injected. This resistance change shows that the magnetization of the FL1 was switched from up to down, corresponding to the antiparallel configuration. In the bit shifting experiment, we injected pulse currents in the -z direction into the nanopillar without external magnetic field and observed a sudden decrease in resistance at a current pulse of -18 mA, which indicates that the magnetization switched to a parallel state. This result corresponds to the process of shifting the data from the FL1 to the FL2, and the magnetization of the free layers became down-down magnetization configuration. Finally, by sweeping the out-of-plane magnetic field from 0 to +200 mT on the final state of the bit shifting process, we observed the magnetization transitioning from parallel to antiparallel and then back to parallel. Therefore, we confirm the final state of the bit shift is down-down, which aligns with our expected experimental results. Similar results were observed in the bit writing and shifting experiments starting from the down-down magnetization configuration. Thus, data-writing and shifting operations from different initial states are achieved in this double free layer nanopillar.

III. CONCLUSION

In summary, we fabricated a 300 nm diameter nanopillar with double free layers, and achieved data write and shift. The data-writing step is achieved by SOT magnetization switching of the lower free layer assisted by a tilted magnetic field. The written data was shifted to the upper free layer by STT induced by out-of-plane current pulse injection. However, these devices do have some limitations. For example, in our experiments, the SOT-induced magnetization switching requires the application of an external magnetic field, and the currents used for writing and shifting remain relatively high. This suggests that further research is needed regarding the field-free writing method [26]-

[29], material selection [15], [16], and structural optimization. Despite these drawbacks, this study still suggests that the concept of vertical DW motion memory proposed in our previous research is feasible. We believe the data writing and shifting processes conducted using our double free layer memory cell could provide valuable insights for the development of DW motion memory and facilitate advancements in next-generation memory technologies.

REFERENCES

[1] S. Parkin, X. Jiang, C. Kaiser, A. Panchula, K. Roche, and M. Samant, "Magnetically engineered spintronic sensors and memory," *Proc. IEEE*, vol. 91, pp. 661-680, May 2003.

[2] S. Parkin, M. Hayashi, and L. Thomas, "Magnetic domain-wall racetrack memory," *Science,* vol. 320, pp. 190-194, Apr. 2008.

[3] S.-H. Yang, K.-S. Ryu, and S. Parkin, "Domain-wall velocities of up to $750 \mathrm{~m~s}^{-1}$ driven by exchange-coupling torque in synthetic antiferromagnets," *Nat. Nanotechnol.*, vol. 10, pp. 221-226, Jan. 2015.

[4] J. C. Slonczewski, "Current-driven excitation of magnetic multilayers," *J. Magn. Magn. Mater.*, 159, pp. L1-L7, June 1996.

[5] L. Berger, "Emission of spin waves by a magnetic multilayer traversed by a current," *Phys. Rev. B*, vol. 54, p. 9353, Oct. 1996.

[6] D. C. Ralph and M. D. Stiles, "Spin transfer torques," *J. Magn. Magn. Mater.*, vol. 320, pp. 1190-1216, Apr. 2008.

[7] A. Yamaguchi, T. Ono, S. Nasu, K. Miyake, K. Mibu, and T. Shinjo, "Real-space observation of current-driven domain wall motion in submicron magnetic wires," *Phys. Rev. Lett.*, vol. 92, p. 077205, Feb. 2004.

[8] K. -J. Kim, R. Hiramatsu, T. Koyama, K. Ueda, Y. Yoshimura, D. Chiba, K. Kobayashi, Y. Nakatani, S. Fukami, M. Yamanouchi, H. Ohno, H. Kohno, G. Tatara, and T. Ono, "Two-barrier stability that allows low-power operation in current-induced domain-wall motion," *Nat. Commun.*, vol. 4, p. 2011, June 2013.

[9] M. Lundstrom, "Moore's law forever?" *Science*, vol. 299, pp. 210-211, Jan. 2003.

[10] H. N. Khan, D. A. Hounshell, and E. R. H. Fuchs, "Science and research policy at the end of Moore's law," *Nat. Electron.*, vol. 1, pp. 14–21, Jan. 2018.

[11] A. Manchon, J. Železný, I. M. Miron, T. Jungwirth, J. Sinova, A. Thiaville, K. Garello, and P. Gambardella, "Current-induced spin-orbit torques in ferromagnetic and antiferromagnetic systems," *Rev. Mod. Phys.*, vol. 91, p. 035004, Sept. 2019.

[12] J. Sinova, S. O. Valenzuela, J. Wunderlich, C. H. Back, and T. Jungwirth, "Spin Hall effects," *Rev. Mod. Phys.*, vol. 87, p. 1213, Oct. 2015.

[13] T. Taniguchi, S. Mitani, and M. Hayashi, "Critical current destabilizing perpendicular magnetization by the spin Hall effect," *Phys. Rev. B*, vol. 92, p. 024428, July 2015.

[14] P. Gambardella and I. M. Miron, "Current-induced spin–orbit torques," *Phil. Trans. R. Soc. A*, vol. 369, pp. 3175-3197, Aug. 2011.

[15] Y. M. Hung, T. Li, R. Hisatomi, Y. Shiota, T. Moriyama, and T. Ono, "Low current driven vertical domain wall motion memory with an artificial ferromagnet," *J. Magn. Soc. Jpn.*, vol. 45, pp. 6-11, Jan. 2021.

[16] Y. M. Hung, Y. Shiota, R. Hisatomi, T. Moriyama, and T. Ono, "High thermal stability and low driven current achieved by vertical domain wall

[17] J. H. Lee, D. Petit, R. Lavrijsen, A. Fernández-Pacheco, R. Mansell, and R. P. Cowburn, "Soliton propagation in micron-sized magnetic ratchet elements," *Appl. Phys. Lett.*, vol. 104, p. 232404, June 2014.

[18] R. Lavrijsen, J. H. Lee, A. Fernández-Pacheco, D. Petit, R. Mansell, and R. P. Cowburn, "Magnetic ratchet for three-dimensional spintronic memory and logic," *Nature*, vol. 493, pp. 647-650, Jan. 2013.

[19] K. Y. Camsari, M. M. Torunbalci, W. A. Borders, H. Ohno, and S. Fukami, "Double-free-layer magnetic tunnel junctions for probabilistic bits," *Phys. Rev. Applied*, vol. 15, p. 044049, Apr. 2021.

[20] K. Selcuk, S. Kanai, R. Ota, H. Ohno, S. Fukami, and K. Y. Camsari, "Double-free-layer stochastic magnetic tunnel junctions with synthetic antiferromagnets," *Phys. Rev. Applied*, vol. 21, p. 054002, May 2024.

[21] L. Farcis, B. M. S. Teixeira, P. Talatchian, D. Salomoni, U. Ebels, S. Auffret, B. Dieny, F. A. Mizrahi, J. Grollier, R. C. Sousa, and L. D. Buda-Prejbeanu, "Spiking Dynamics in Dual Free Layer Perpendicular Magnetic Tunnel Junctions," *Nano Letters*, vol. 23, no. 17, pp. 7869-7875, Aug. 2023.

[22] G. Y. Guo, S. Murakami, T.-W. Chen, and N. Nagaosa, "Intrinsic spin Hall effect in Platinum: First-principles calculations," *Phys. Rev. Lett.*, vol. 100, p. 096401, Mar. 2008.

[23] I. M. Miron, K. Garello, G. Gaudin, P. -J. Zermatten, M. V. Costache, S. Auffret, S. Bandiera, B. Rodmacq, A. Schuhl, and P. Gambardella, "Perpendicular switching of a single ferromagnetic layer induced by in-plane current injection," *Nature*, vol. 476, pp. 189-193, July 2011.

[24] L. Liu, O. J. Lee, T. J. Gudmundsen, D. C. Ralph, and R. A. Buhrman, "Current-induced switching of perpendicularly magnetized magnetic layers using spin torque from the spin Hall effect," *Phys. Rev. Lett.*, vol. 109, p. 096602, Aug. 2012.

[25] K. Garello, I. M. Miron, C. O. Avci, F. Freimuth, Y. Mokrousov, S. Blügel, S. Auffret, O. Boulle, G. Gaudin, and P. Gambardella, "Symmetry and magnitude of spin–orbit torques in ferromagnetic heterostructures," *Nat. Nanotechnol.*, vol. 8, pp. 587-593, July 2013.

[26] G. Yu, P. Upadhyaya, Y. Fan, J. G. Alzate, W. Jiang, K. L. Wong, S. Takei, S. A. Bender, L. -T. Chang, Y. Jiang, M. Lang, J. Tang, Y. Wang, Y. Tserkovnyak, P. K. Amiri, and K. L. Wang, "Switching of perpendicular magnetization by spin–orbit torques in the absence of external magnetic fields," *Nat. Nanotechnol.*, vol. 9, pp. 548-554, May 2014.

[27] S. Fukami, C. L. Zhang, S. DuttaGupta, A. Kurenkov, and H. Ohno, "Magnetization switching by spin–orbit torque in an antiferromagnet–ferromagnet bilayer system," *Nat. Mater.*, vol. 15, pp. 535-541, Feb. 2016.

[28] Y.-C. Lau, D. Betto, K. Rode, J. M. D. Coey, and P. Stamenov, "Spin–orbit torque switching without an external field using interlayer exchange coupling," *Nat. Nanotechnol.*, vol. 11, pp. 758-762, May 2016.

[29] Y. Liu, G. Shi, D. Kumar, T. Kim, S. Shi, D. Yang, J. Zhang, C. Zhang, F. Wang, S. Yang, Y. Pu, P. Yu, K. Cai, and H. Yang, "Field-free switching of perpendicular magnetization at room temperature using out-of-plane spins from $TaIrTe_4$," *Nat. Electron.*, vol. 6, pp. 732-738, Oct. 2023.

motion memory with artificial ferromagnet," *Appl. Phys. Express*, vol. 14, p. 023001, Jan. 2021.
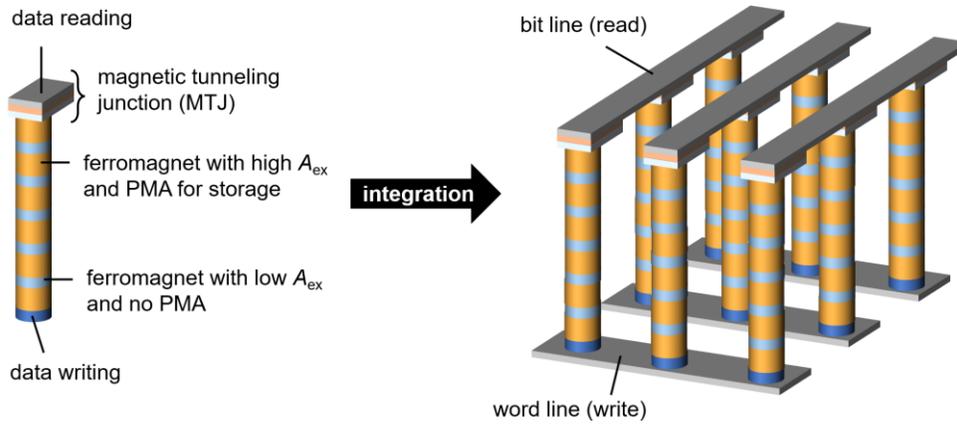
Fig. 1 A vertical domain wall motion memory cell with perpendicular magnetic anisotropy. Here, A_{ex} refers to magnetic exchange stiffness. In this memory structure, ferromagnets with high A_{ex} and PMA are used to store digital bits, while those with low A_{ex} and no PMA are used to carry DWs.
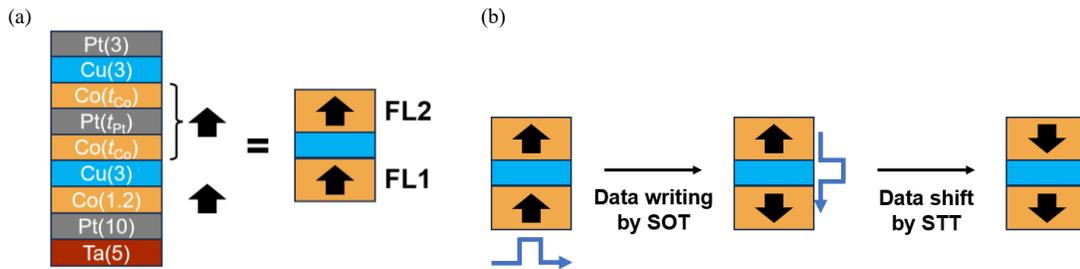
(a)

(b)

Fig. 2 (a) A schematic illustration of the multilayer structure. (b) Memory operations of the double-free-layer nanopillar.
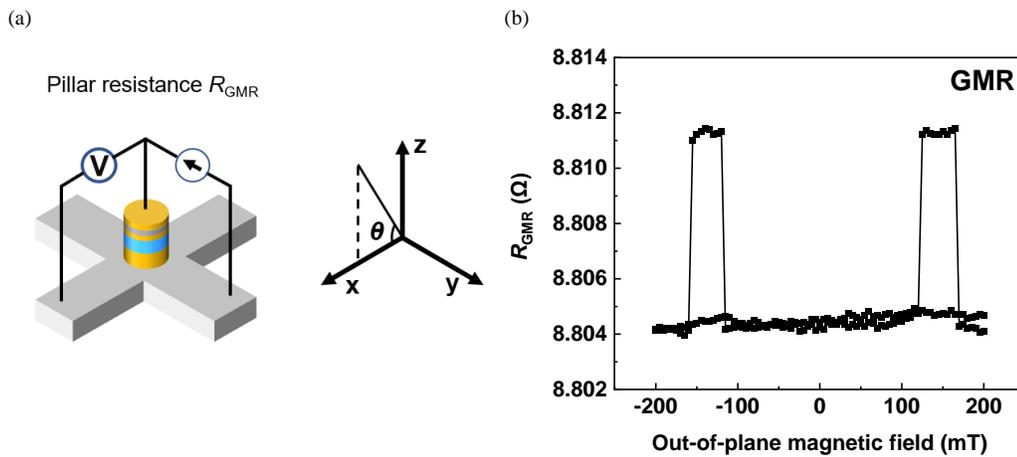
(a)

(b)

Fig.3 (a) Schematic of the experimental setup for the GMR measurement and the coordinate system. (b) The resistance-field loops of the device with $t_{Co} = 0.35$ nm, and $t_{Pt} = 0.75$ nm.
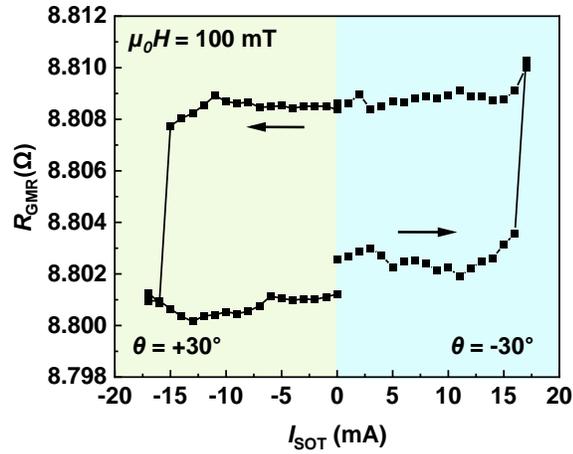
Fig. 4 SOT switching loops are measured by GMR effect. The elevation angle θ of the applied magnetic field was set to -30° when +x current pulses are injected, and switched to +30° when the current pulses are in the -x direction.
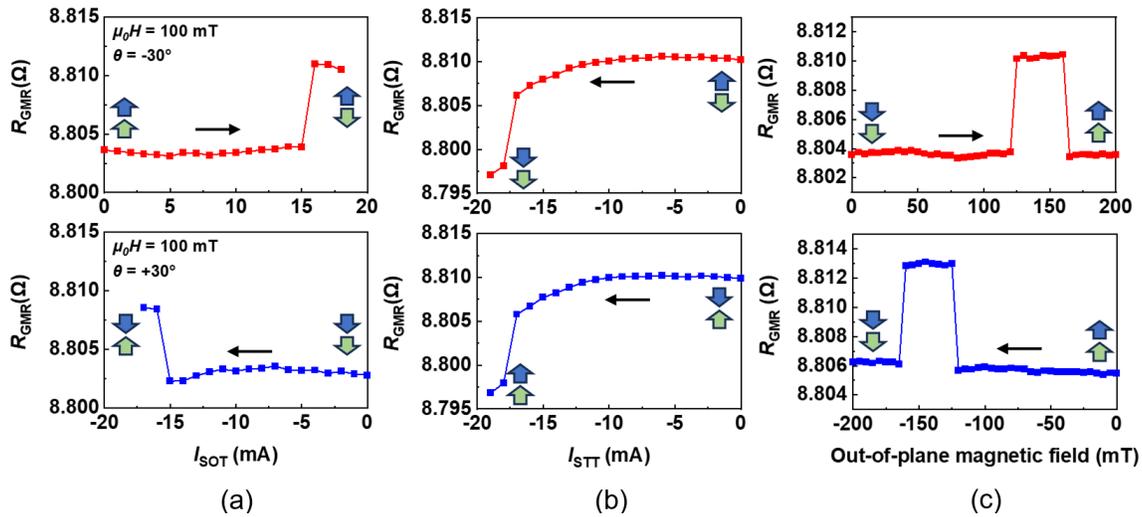

Fig. 5 The data-writing (a) and shifting (b) processes are achieved from up-up (red) and down-down (blue) initial states. (c) the final states after bit shifts are confirmed by sweeping an out-of-plane magnetic field.